Electronic Supplementary Material (ESI) for New Journal of Chemistry.

[Supporting Information]

Hydrogen bonding controlled catalysis of a porous organic framework containing benzimidazole moieties

Bing Liu[a], *Teng Ben*[b]*, *Jun Xu*,[c] *Feng Deng*,[c] *Shilun Qiu*[a]*

[a] *State Key Lab of Inorganic Synthesis & Preparative Chemistry, Jilin University, 130012, China. E-mail: sqiu@jlu.edu.cn; Fax: +(86) 431 85168331; Tel: +(86) 431 85168331*

[b] *Department of Chemistry, Jilin University, 130012, China. E-mail: tben@jlu.edu.cn*

[c] *Wuhan Institute of Physics and Mathematics - State Key Laboratory of Magnetic Resonance and Atomic and Molecular Physics, Wuhan, China*

*To whom correspondence should be addressed.

Table of Contents

1. Instruments and Methods

1-1. TGA Experiment.

The thermogravimetric analysis (TGA) was performed using a SHIMADZU DTG-60 thermal analyzer system at the heating rate of 10 ^{o}C min^{-1} to 800 ^{o}C in the dried air atmosphere and the air flow rate was 30 mL min^{-1}. The sample was loaded in alumina pan.

1-2. FT-IR Experiment.

The FTIR spectra (KBr, Aldrich) were measured using a BRUKER VERTEX 80V Fourier transform infrared spectrometer. Samples were packed firmly to get transparent films. Measurements were carried out under vacuum to decrease the interference of moisture.

1-3. Elemental Analysis.

Elemental analysis was performed using an Elementar Vario EL cube.

1-4. PXRD Experiment.

PXRD measurements were performed using a SHIMADZU XRD-6000 X-ray diffractometer using Cu-Kα radiation, 40 kV, 30 mA with a scanning rate of 0.15° min^{-1} (2θ).

1-5. SEM and EDS analysis.

The sample was prepared by dispersing the material onto a sticky carbon surface attached to a flat aluminum sample holder. Scanning electron microscopy (SEM) was performed on an FEI Quanta 400 Thermal FE Environment Scanning Electron Microscope and energy dispersive spectrometer (EDS) analysis was performed on a JEOS JSM 6700.

1-6. ^{1}H NMR and ^{13}C CP-MAS NMR analysis.

We use a BRUKER NMR (400 MHz) to perform ^{1}H NMR of products of catalytic reaction. Solid state NMR spectroscopy experiment was carried out at 9.4 T with a Varian Infinity plus-400 spectrometer, equipped with a Chemagnetic triple-resonance 7.5 mm probe, with resonance frequencies of 100.6 and 161.9 MHz for ^{13}C. The MAS rate was set to 3–5 kHz. For the ^{1}H-^{13}C cross-polarization (CP)/MAS NMR experiments, the Hartmann–Hahn condition was achieved using hexamethylbenzene (HMB), with a contact time of 2.0 ms and a repetition time of 2.0 s.

1-7. Low-pressure N_2 Sorption measurements.

Nitrogen sorption experiments were performed at 77 K up to 1 bar using a Micro Meritics Tristar II 3020 surface area and pore size analyzer. Before sorption analysis, the sample was evacuated at 150 °C for 10 h using a turbo molecular vacuum pump. Specific surface areas were calculated from nitrogen adsorption data by multipoint BET

analysis. Pore size distributions were calculated from the N_2 adsorption isotherms using non-local density functional theory (NLDFT) method.

1-8. Low-pressure H_2, CO_2 and CH_4 Sorption measurements.

Low-pressure H_2, CO_2 and CH_4 sorption was measured using a Micro Meritics Tristar II 3020 surface area and pore size analyzer. Ultra-high-purity grade H_2, CO_2 (99.999%) and CH_4 gases (99.99%) were used for all adsorption measurements. Free space was measured using helium (99.999%), assuming that the helium is not adsorbed at any of the studied temperatures. H_2 isotherms at 77 K were measured in a liquid nitrogen bath, H_2 isotherms at 87 K were measured in the liquid argon bath, CO_2 and CH_4 isotherms at 273 K were measured in an ice-water bath. To provide high accuracy and precision on determining the relative pressure (P/P_0), the vapor pressure for each data point was monitored throughout the gas sorption analyses.

1-9. HPLC analysis

To analyze the conversion of substrate, part of the mixture was filtered out and the filtration was prepared to be solution for test. Here we use a SHIMADZU LC-10 HPLC with wave length 254 nm.

2. Investigation of Structure of JUC-Z12

2-1. TGA Experiment

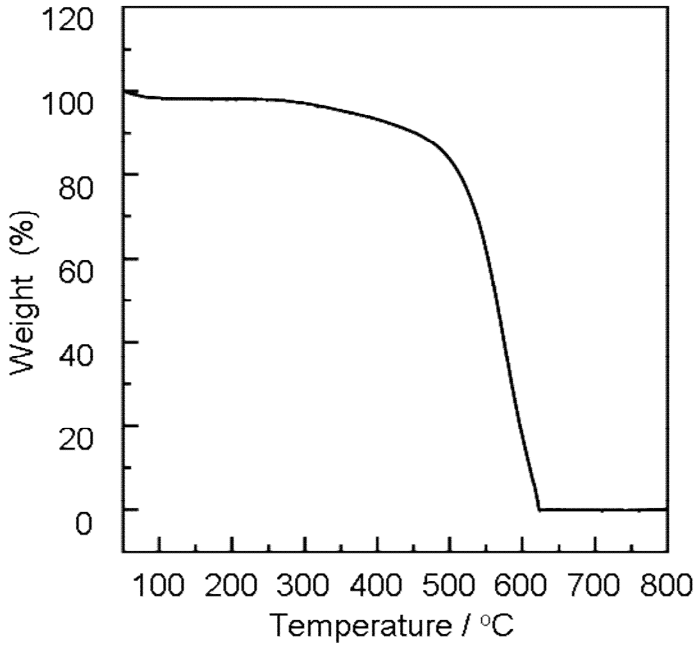

Fig. S1 TGA plot of JUC-Z12 under dry air with the rate of 10 ^{o}C min^{-1}.

2-2. FT-IR of JUC-Z12

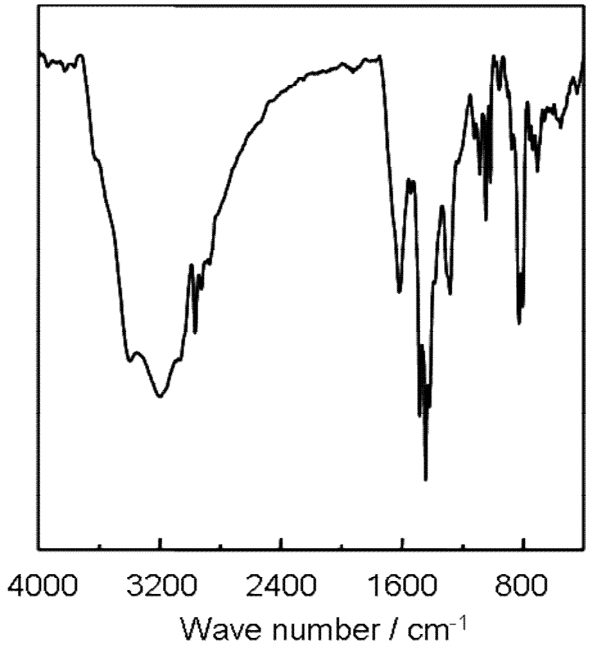

Fig. S2 FT-IR spectra of JUC-Z12.

2-3. PXRD of JUC-Z12

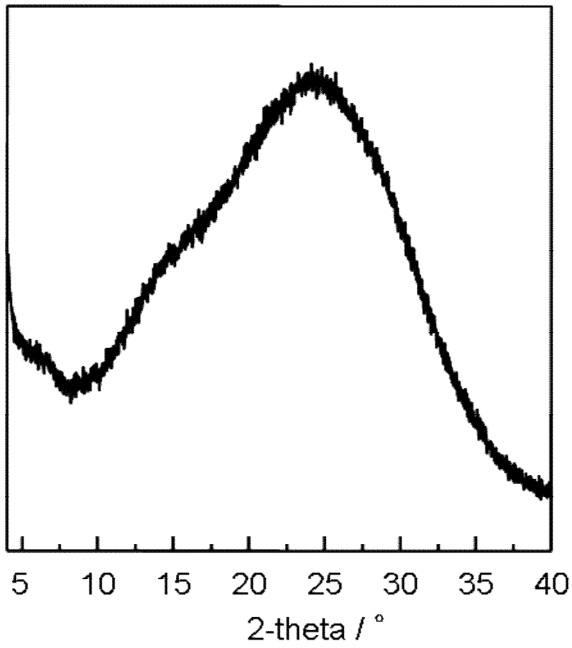

Fig. S3 PXRD pattern of JUC-Z12.

2-4. SEM of JUC-Z12

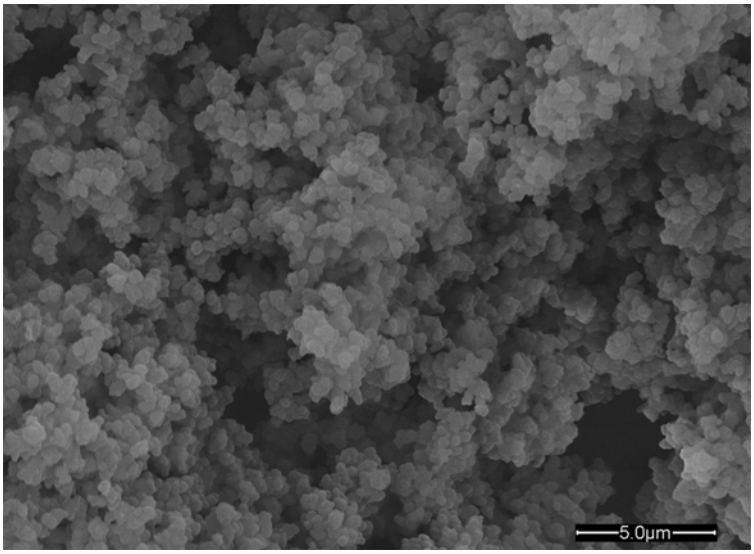

Fig. S4 SEM image of JUC-Z12.

2-5. EDS of JUC-Z12

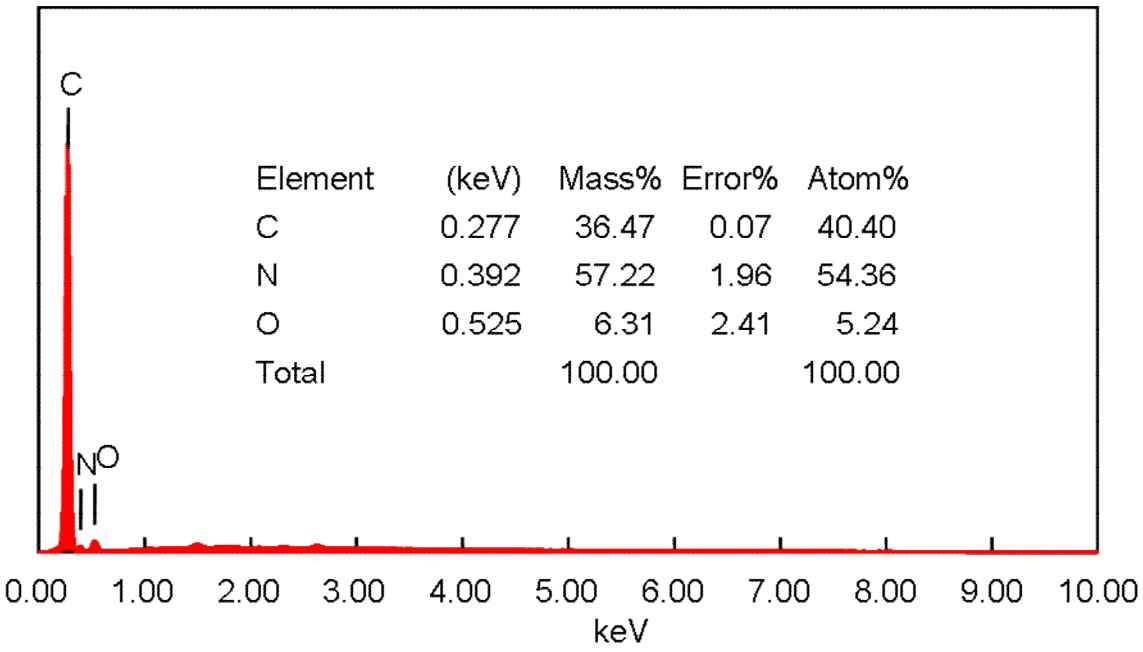

Fig. S5 EDS result of JUC-Z12.

2-6. ^{13}C CP-MAS NMR of JUC-Z12

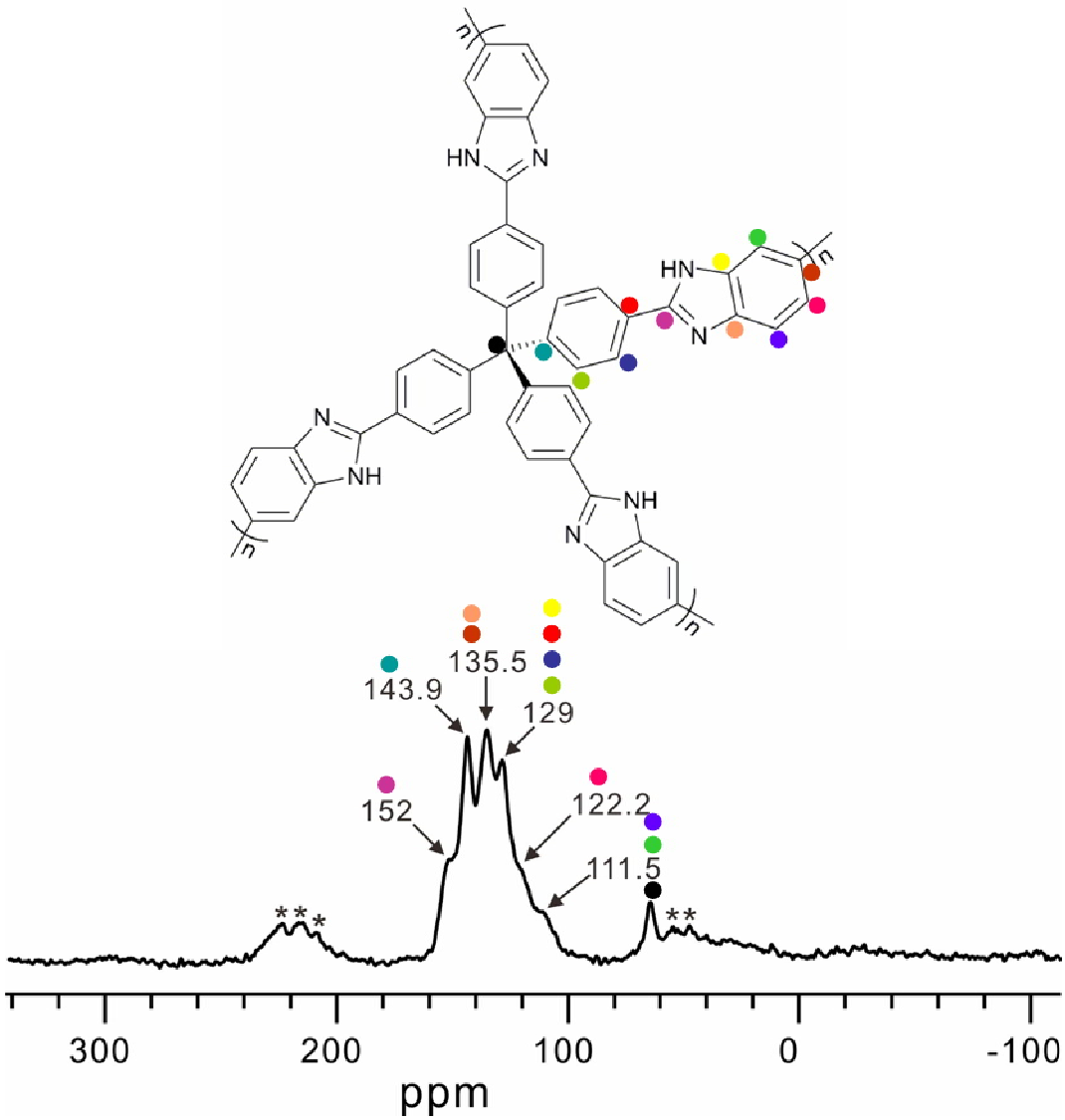

Fig. S6 ^{13}C CP-MAS NMR spectrum of JUC-Z12.

3. Gas Storage

3-1. Investigation of Adsorption of N_2 (77K)

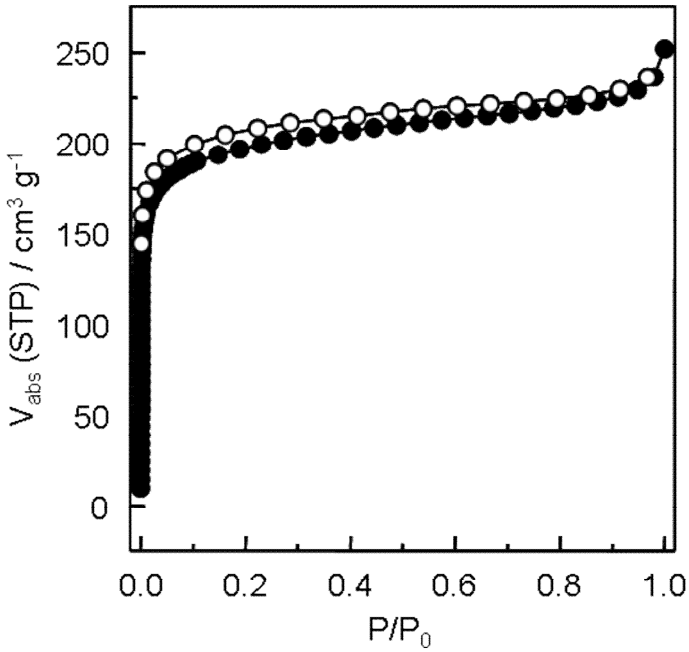

Fig. S7 77 K, N_2 sorption isotherms of JUC-Z12 (solid symbols: adsorption; open symbols: desorption).

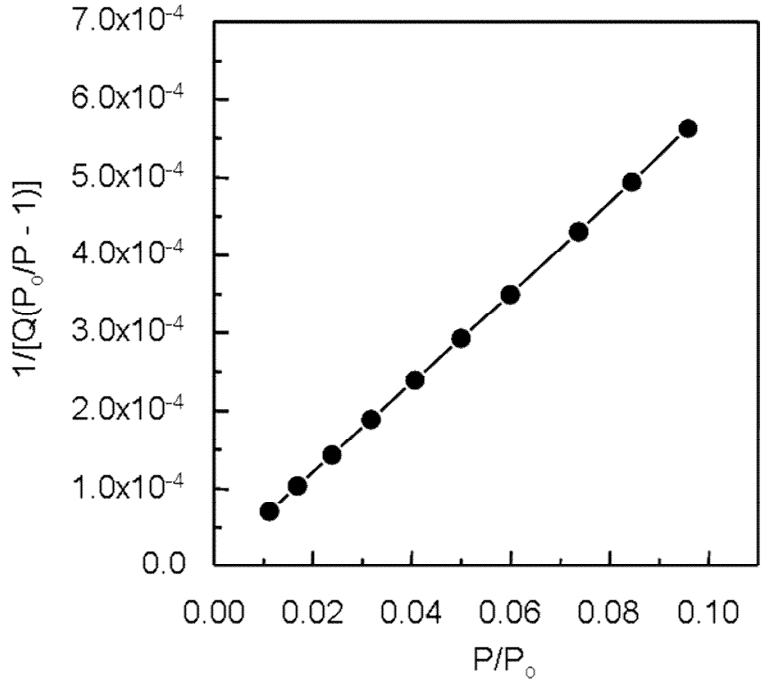

Fig. S8 BET plot derived from N_2 adsorption (R^2 = 0.999934, S_{BET} = 750 m^2 g^{-1}).

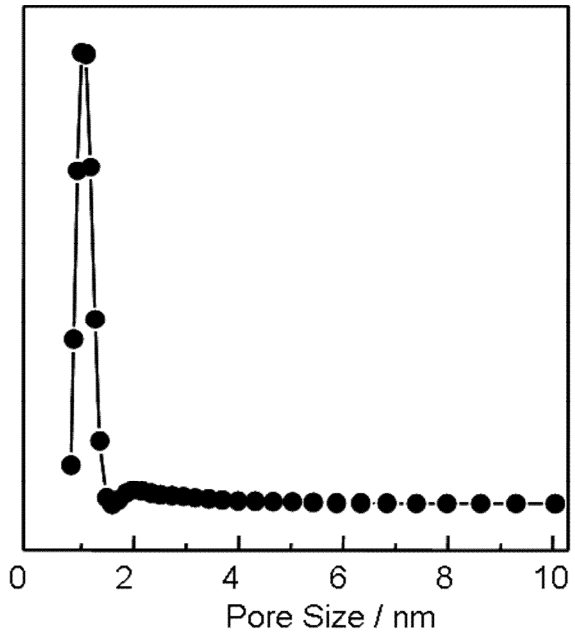

Fig. S9 Pore size distributions derived from N_2 adsorption by DFT.

3-2. Investigation of Adsorption of H_2 (77 K, 87 K)

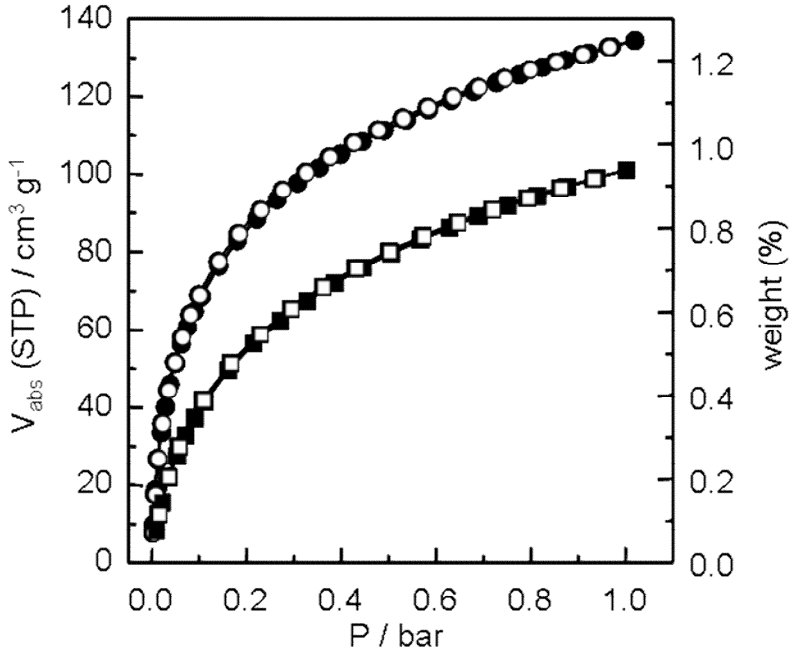

Fig. S10 H_2 adsorption (solid symbols) and desorption (open symbols) isotherms of JUC-Z12 at 77 K (cycle) and 87 K (square).

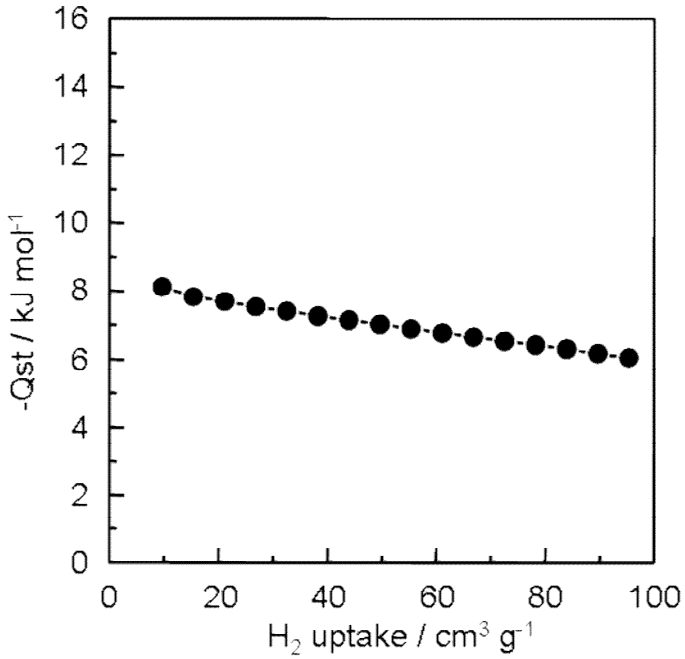

Fig. S11 Qst_{H2} of JUC-Z12 as a function of the amount of H_2 adsorbed.

3-3. Investigation of Adsorption of CH_4 (273 K, 298 K)

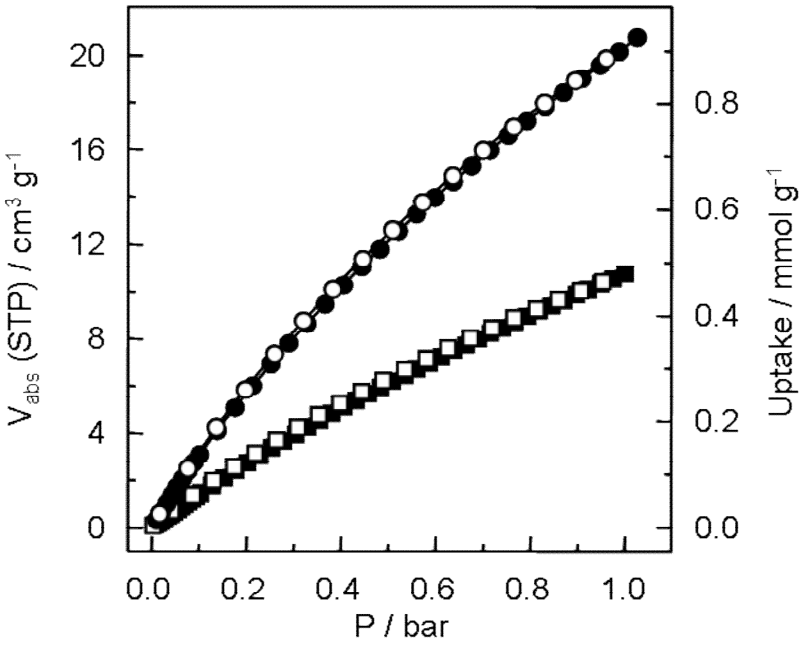

Fig. S12 CH_4 adsorption (solid symbols) and desorption (open symbols) isotherms of JUC-Z12 at 273 K (cycle) and 298 K (square).

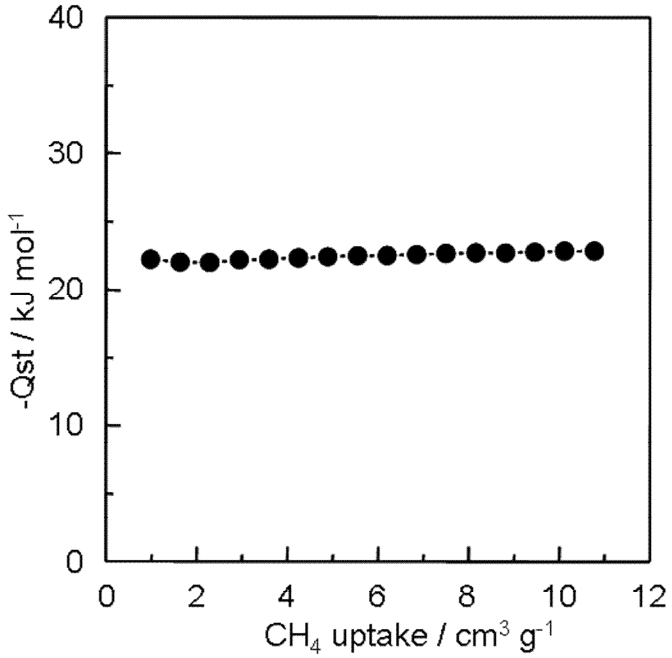

Fig. S13 Qst_{CH4} of JUC-Z12 as a function of the amount of CH_4 adsorbed.

3-4. Investigation of Adsorption of CO_2 (273 K, 298 K)

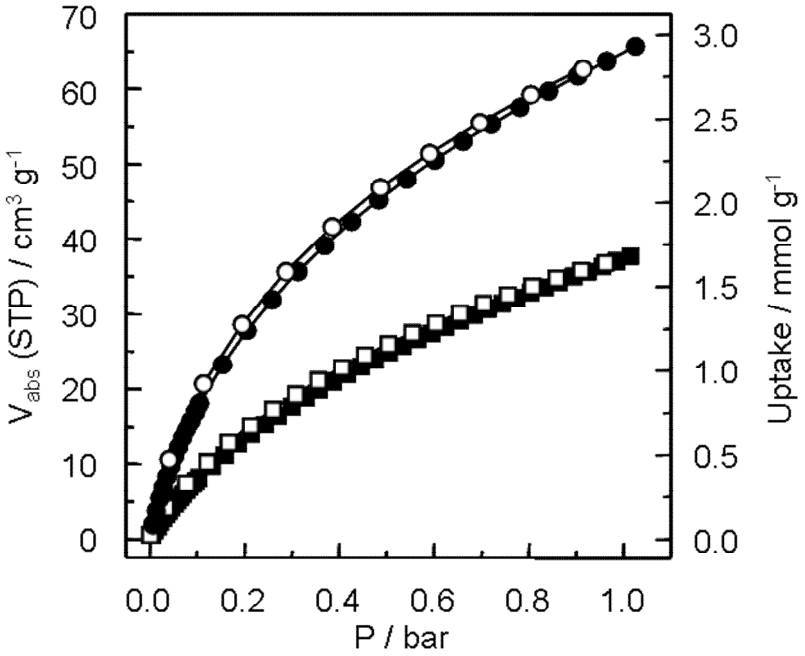

Fig. S14 CO_2 adsorption (solid symbols) and desorption (open symbols) isotherms of JUC-Z12 at 273 K (cycle) and 298 K (square).

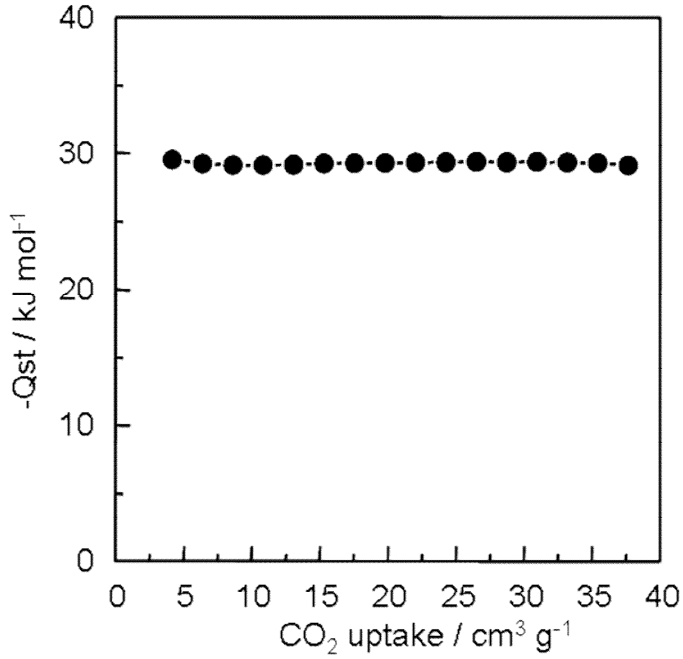

Fig. S15 Qst_{CO2} of JUC-Z12 as a function of the amount of CO_2 adsorbed.

4. Catalytic reactions with JUC-Z12

4-1. ^{1}H-NMR of 4-methylbenzaldehyde and 2-(4-methylbenzylidene)malononitrile

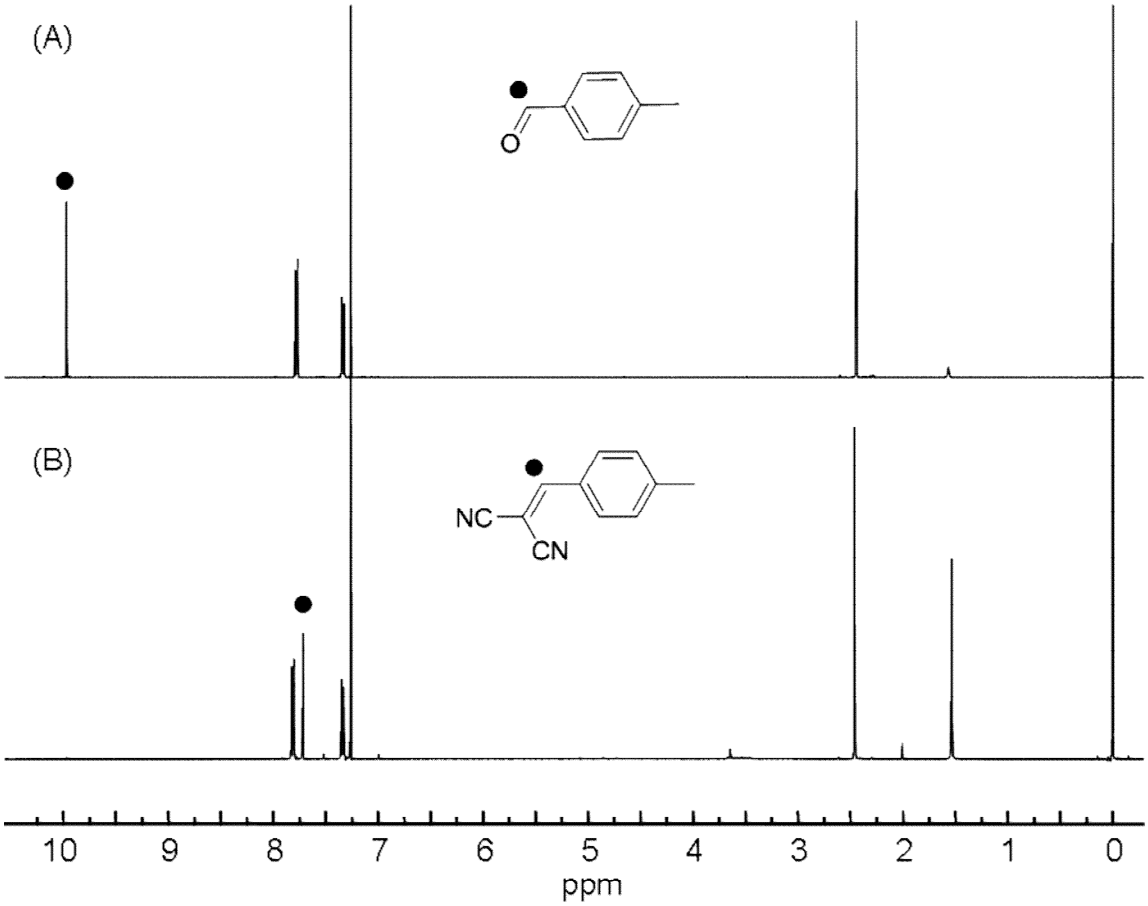

Fig. S16 ^{1}H NMR spectrum of (A) 4-methylbenzaldehyde and (B) 2-(4-methylbenzylidene)malononitrile in $CDCl_3$.

4-2. ^{1}H-NMR of benzaldehyde and 2-benzylidenemalononitrile

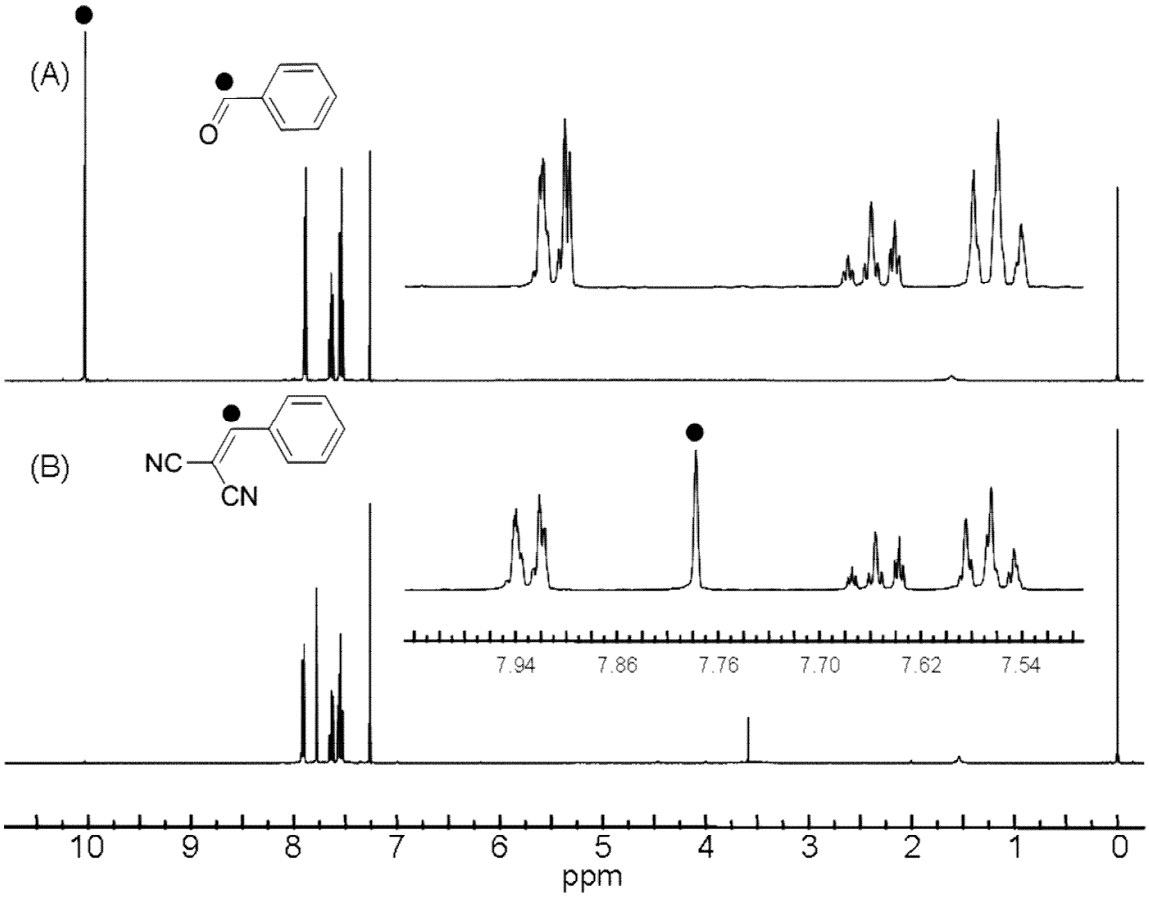

Fig. S17 ^{1}H NMR spectrum of (A) benzaldehyde and (B) 2-benzylidenemalononitrile in $CDCl_3$.

4-3. ^{1}H-NMR of 4-bromobenzaldehyde and 2-(4-bromobenzylidene)malononitrile

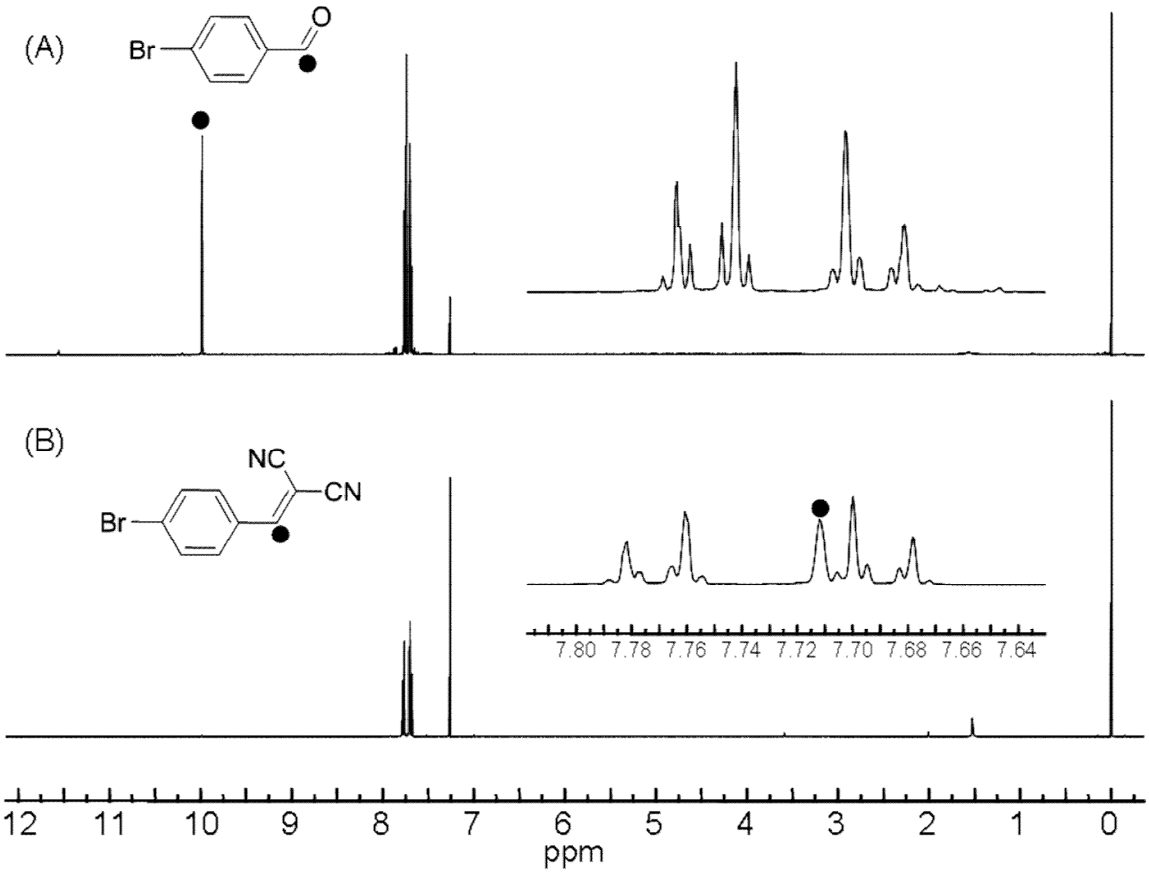

Fig. S18 ^{1}H NMR spectrum of (A) 4-bromobenzaldehyde and (B) 2-(4-bromobenzylidene)malononitrile in $CDCl_3$.

4-4. [1]H-NMR of 4-chlorobenzaldehyde and 2-(4-chlorobenzylidene)malononitrile

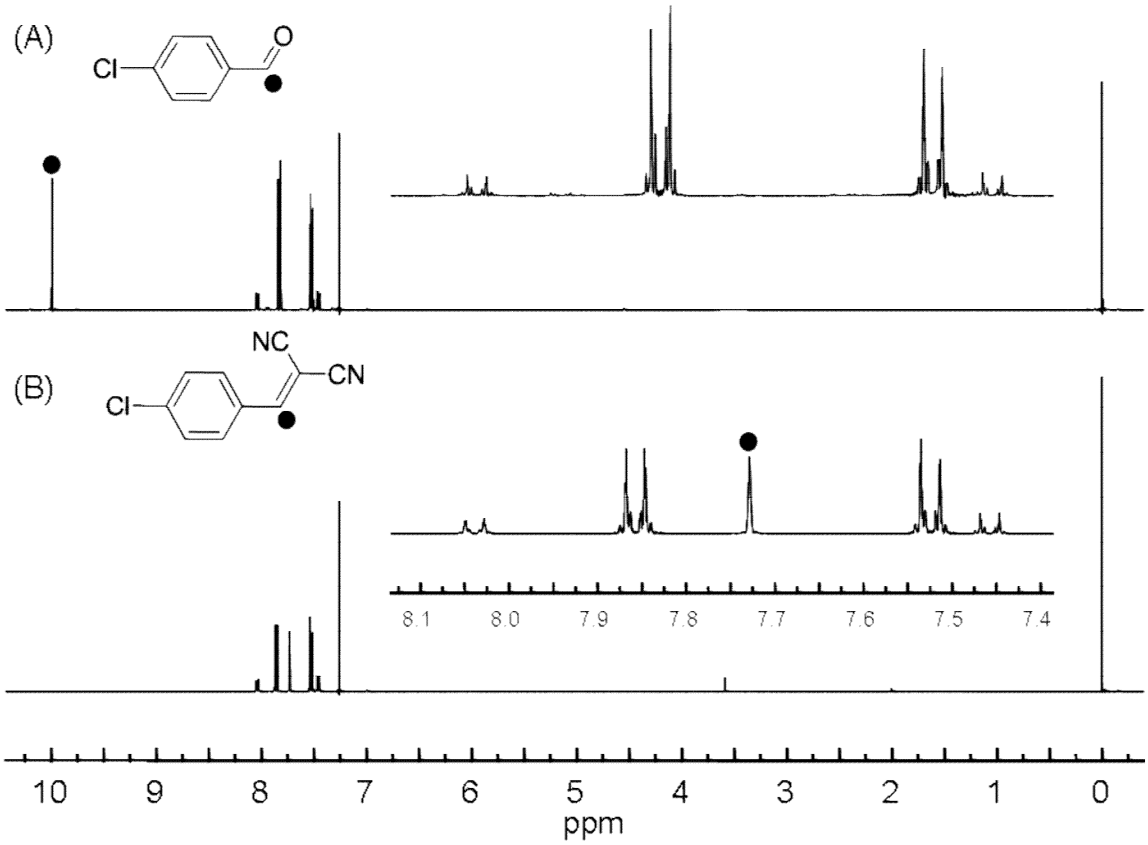

Fig. S19 ^{1}H NMR spectrum of (A) 4-chlorobenzaldehyde and (B) 2-(4-chlorobenzylidene)malononitrile in $CDCl_3$.

4-5. ^{1}H-NMR of 4-methoxybenzaldehyde and 2-(4-methoxybenzylidene)malononitrile

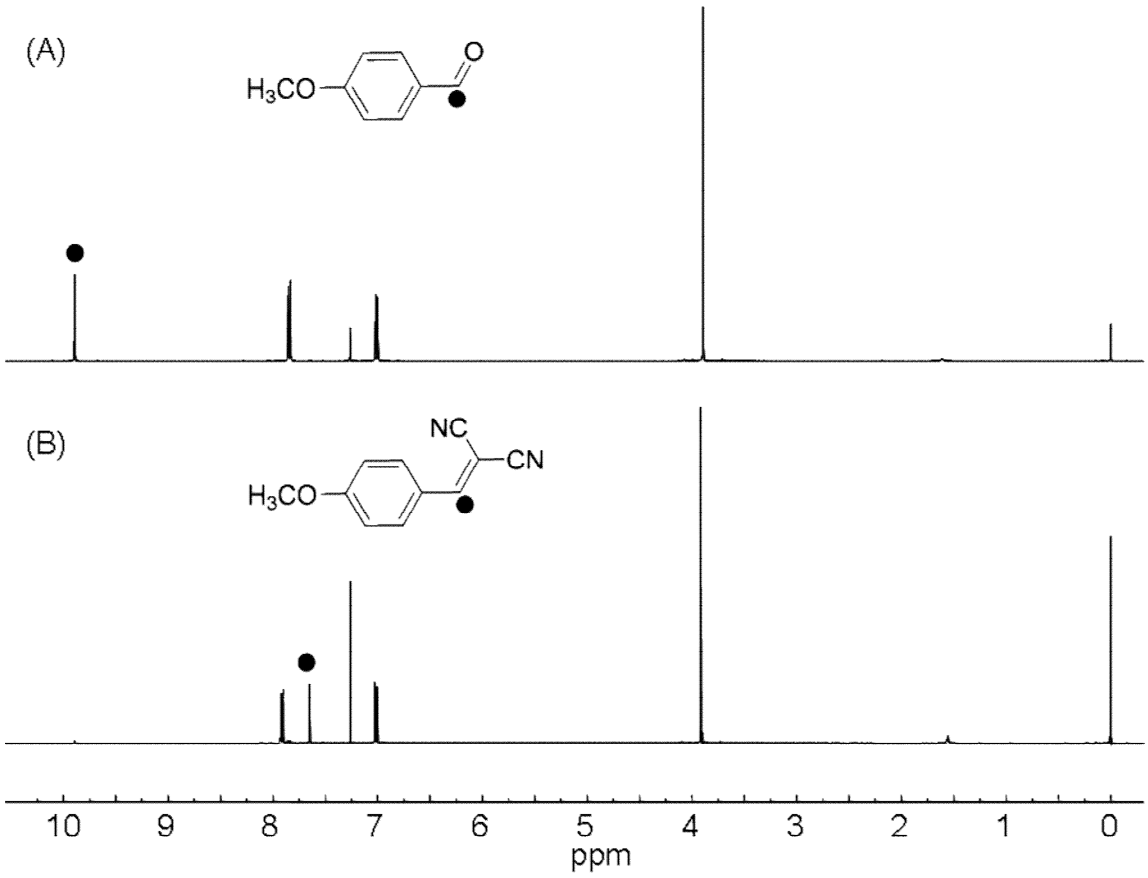

Fig. S20 ^{1}H NMR spectrum of (A) 4-methoxybenzaldehyde and (B) 2-(4-methoxybenzylidene)malononitrile in $CDCl_3$.

4-6. ^{1}H-NMR of 4-hydroxybenzaldehyde and 2-(4-hydroxybenzylidene)malononitrile

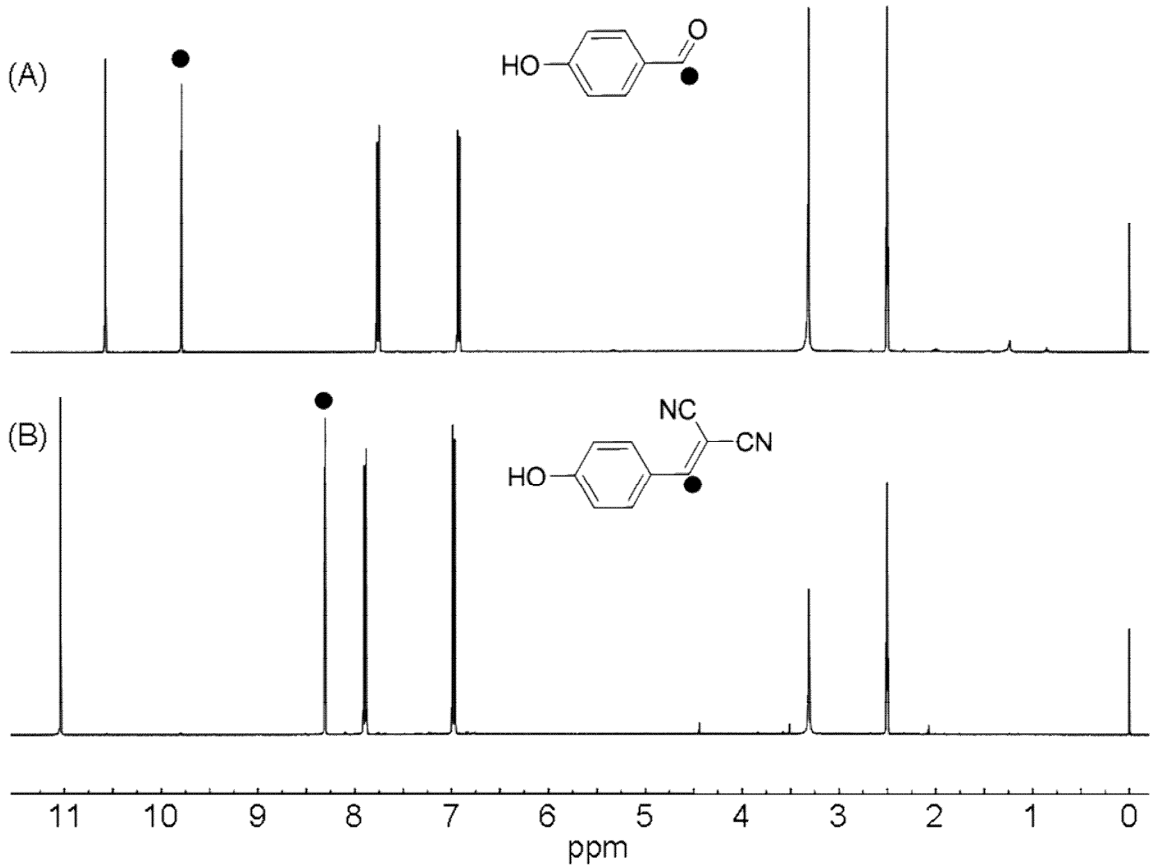

Fig. S21 ^{1}H NMR spectrum of (A) 4-hydroxybenzaldehyde and (B) 2-(4-hydroxybenzylidene)malononitrile in d_6-DMSO.